Structure and Properties of *N*,*N*-Alkylene Bis(*N*′-Alkylimidazolium) Salts

Minjae Lee, Zhenbin Niu, Carla Slebodnick, and Harry W. Gibson*

Department of Chemistry, Virginia Polytechnic Institute & State University, Blacksburg, Virginia 24061

Received: March 15, 2010; Revised Manuscript Received: April 22, 2010

A series of *N*,*N*-alkylene bis(*N*′-alkylimidazolium) salts with various anions was prepared and characterized. The hydrogen-bonding abilities and ion-pairing strengths of the salts in solution were varied by changing the solvent and anion. Qualitatively, the extent of ion pairing of the 1,2-bis[*N*-(*N*′-butylimidazolium)]ethane salts with different anions was determined in acetone-d_6 by ^{1}H NMR spectroscopy. Thermal properties of the imidazolium salts were related not only to the nature of anions but also to the spacer length between imidazolium cations. Exceptionally high melting points of 1,2-bis[*N*-(*N*′-alkylimidazolium)]ethane bis(hexafluorophosphate)s can be explained by multiple hydrogen bonds observed in the X-ray crystal structures. Moreover, a *trans* conformation of the ethylene spacer of 1,2-bis[*N*-(*N*′-alkylimidazolium)]ethane bis(hexafluorophosphate)s allows good stacking structure in the crystals.

Introduction

Imidazolium salts are well-known *N*-heterocyclic carbene (NHC) precursors in organometallic chemistry[1−11] and homogeneous catalysis.[12−15] The formation of NHC is due to the acidic proton on the 2-position of the imidazolium unit; its pK_a is 16−24, which depends on the nature of the substituents on the two imidazolium nitrogens.[16] Anions of the imidazolium salts also have a strong influence on the H/D exchange reaction at the 2-position; for example, the 1-butyl-3-methyl dicyanimide salt undergoes deuterium exchange even in the absence of any base.[17] Transition-metal complexes with bis(alkylimidazolium) salts containing a $(CH_2)_n$ linker were studied; the length of the linker controls physical properties and effects the chelating ability.[2,5]

Imidazolium salts are also popular as ionic liquids (ILs) because of their unique characteristics, such as low volatility, nonflammability, large electrochemical window, and high ionic conductivity.[18−23] As a result, many new ILs have been synthesized, and applications of ILs have been also expanded in diverse areas, such as electroactive devices.[24−27] Demand for new ILs with designed properties is growing because of the expansion of their applications. As one trend for new imidazolium ILs, systems with more than one imidazolium unit per molecule have been studied to obtain better properties and wider applications. Armstrong et al. studied the structure−property relationships of thermally stable dicationic ILs; the geminal imidazolium dicationic salts, in which two imidazolium units are connected by C_3−C_{12} alkylenes, are more thermally stable than monoimidazolium ILs.[28] Also, the thermal properties and ionic conductivity of imidazolium dicationic di[bis(trifluoromethanesulfonyl)imide] ($2Tf_2N^-$) salts were investigated by Pitawala et al.[29] They compared DSC transitions and ionic conductivities of 2H- (unsubstituted at C2 of imidazolium), 2-methyl-, and 2-phenyl-imidazolium dicationic salts with various spacers, with monoimidazolium Tf_2N^- salts. The applications of imidazolium dicationic salts were also reported; for example, dicationic imidazolium iodide salts with alkylene or ethyleneoxy spacers were used in dye sensitized solar cells,[30,31] and dicationic imidazolium ILs connected with fluoroalkyl, ethyleneoxy, and phenylene units were synthesized as high-temperature lubricants.[32,33]

However, we are surprised that no one has reported a detailed property study of dicationic imidazolium salts with an ethylene spacer. Therefore, here, we report the structure−property relationships of alkylene bis[*N*-(*N*′-alkylimidazolium)] salts with with a C_2 (ethylene) spacer and the comparison of these salts with the analogous salts with C_3 and C_4 spacers with various lengths of *N*-alkyl side chains. We also studied the counterion effects on the properties. Some interesting solid-state structures were found for the imidazolium salts, which showed unique stacking patterns in X-ray crystal structures.

Experimental Section

NMR spectra for all synthesized compounds and X-ray crystallographic data are presented in the Supporting Information.

Materials. Acetone for the quaternization reactions was dried with anhydrous $CaSO_4$ and then distilled. Acetonitrile (MeCN) was dried with anhydrous K_2CO_3 and then distilled. All other chemicals and solvents were used as received.

Instruments. ^{1}H and ^{13}C NMR spectra were obtained on Varian Inova 400 MHz and Unity 400 MHz spectrometers. High-resolution electrospray ionization time-of-flight mass spectrometry (HR ESI TOF MS) was carried out on an Agilent 6220 Accurate Mass TOF LC/MS Spectrometer in positive ion mode. DSC results were obtained on a TA Instrument Q2000 differential scanning calorimeter at a scan rate of 5 or 10 °C/min heating under N_2 purge. TGA results were obtained on a TA Instrument Q500 Thermogravimetric Analyzer at a heating rate of 10 °C/min under N_2 purge. Melting points were observed on a Büchi B-540 apparatus at a 2 °C/min heating rate.

General Anion-Exchange Procedure A. Into a solution of bromide salt (1 equivalent) in deionized water, KPF_6 (or $NaBF_4$ or $LiTf_2N$, 2−4 equivalents) was added with stirring, which continued for 1−2 h at room temperature. The precipitate was filtered and washed with deionized water twice. Drying in a vacuum oven gave the pure imidazolium PF_6^- (or BF_4^- or Tf_2N^-) salt.

* Corresponding author. E-mail: hwgibson@vt.edu; FAX: 540-231-8517; Tel: 540-231-5902.

10.1021/jp102370j
Published on Web 05/06/2010

General Anion-Exchange Procedure B. Into a solution of bromide salt (1 equivalent) in deionized water, AgTfO (or $AgNO_3$ or AgTFA, 2.06 equivalents) was added with stirring, which continued for 3−4 h at 50 °C. Insoluble AgBr was removed by filtration, and the water in the filtrate was removed under vacuum. Further drying in a vacuum oven gave the corresponding TfO^- (or NO_3^- or TFA^-) salt.

1,2-Bis[*N*-(*N*′-methylimidazolium)]ethane Salts (1Br and 1PF$_6$). A solution of 1-methylimidazole (2.49 g, 30 mmol) and 1,2-dibromoethane (2.82 g, 15 mmol) in MeCN (20 mL) was refluxed for three days. The precipitate was filtered after cooling and washed with tetrahydrofuran (THF) three times. Drying in a vacuum oven gave colorless crystalline **1Br** (4.54 g, 86%), mp 231.1−233.8 °C (lit. mp = 230−234 °C).[4] **1PF$_6$** was obtained by following general anion-exchange procedure A; from **1Br** (4.50 g), KPF_6 (5.52 g, 30 mmol), and deionized water (40 mL), colorless crystalline solid **1PF$_6$** (5.26 g, 73% based on 1,2-dibromoethane), mp 213.8−214.9 °C, was isolated. ^{1}H NMR (400 MHz, CD_3CN, 23 °C): δ 3.85 (s, 6H), 4.62 (s, 4H), 7.33 (t, J = 2, 2H), 7.42 (t, J = 2, 2H), 8.40 (s, 2H). ^{13}C NMR (100 MHz, CD_3CN, 23 °C): δ 37.2, 49.7, 123.5, 125.6, 137.6. HRMS (ESI): m/z 337.1022 ($[M-PF_6]^+$, calcd for $C_{10}H_{16}N_4PF_6$ 337.1017, error 1.5 ppm).

1,4-Bis[*N*-(*N*′-methylimidazolium)]butane Salts (2Br and 2PF$_6$). The same procedure as for **1Br** was used. 1-Methylimidazole (2.46 g, 30 mmol) and 1,4-dibromobutane (3.24 g, 15 mmol) in MeCN (20 mL) produced colorless crystalline **2Br** (3.04 g, 53%), mp 131.7−133.8 °C. ^{1}H NMR (400 MHz, D_2O, 23 °C): δ 1.89 (m, 4H), 3.88 (s, 6H), 4.23 (m, 4H), 7.43 (t, J = 2, 2H), 7.46 (t, J = 2, 2H), 8.72 (s, 2H). The ^{1}H NMR spectrum was identical to that in the literature.[34] **2PF$_6$** was obtained by following the general anion-exchange procedure A; from **2Br** (2.10 g, 5.5 mmol), KPF_6 (3.04 g, 16.5 mmol), and deionized water (40 mL), colorless crystalline **2PF$_6$** (2.59 g, 92% from **2Br**), mp 111.7−114.2 °C, resulted. ^{1}H NMR (400 MHz, acetone-d_6, 23 °C): δ 2.05 (t, J = 7, 4H), 4.01 (s, 6H), 4.41 (s, 4H), 7.66 (t, J = 2, 2H), 7.68 (t, J = 2, 2H), 8.86 (s, 2H). ^{13}C NMR (100 MHz, acetone-d_6, 23 °C): δ 26.7, 35.9, 49.0, 122.6, 124.2, 136.7. HRMS (ESI): m/z calcd 365.1344 ($[M-PF_6]^+$, calcd for $C_{12}H_{20}N_4PF_6$ 365.1330, error 3.8 ppm).

1,2-Bis[*N*-(*N*′-butylimidazolium)]ethane Dibromide (3Br). The same procedure as for **1Br** was used. From 1-butylimidazole (6.21 g, 50 mmol) and 1,2-dibromoethane (4.69 g, 25 mmol) in MeCN (25 mL), colorless crystalline **3Br** (9.64 g, 88%), mp 166.5−168.2 °C, was produced. ^{1}H NMR (400 MHz, D_2O, 23 °C): δ 0.90 (t, J = 7, 6H), 1.25 (m, 4H), 1.83 (m, 4H), 4.22 (t, J = 7, 4H), 4.80 (s, 4H), 7.52 (t, J = 2, 2H), 7.62 (t, J = 2, 2H), 8.85 (s, 2H). The ^{1}H NMR result corresponds to the literature spectrum (in $CDCl_3$).[5] HRMS (ESI): m/z 355.1508 ($[M-Br]^+$, calcd for $C_{16}H_{28}N_4Br$ 355.1497, error 3.1 ppm).

1,2-Bis[*N*-(*N*′-butylimidazolium)]ethane Bis(hexafluorophosphate) (3PF$_6$). Anion-exchange procedure A was used; from **3Br** (1.30 g, 3.0 mmol) and KPF_6 (1.65 g, 9 mmol) in deionized water (10 mL), colorless crystalline **3PF$_6$** (1.54 g, 91%), mp 181.6−182.5 °C, was isolated. ^{1}H NMR (400 MHz, acetone-d_6, 23 °C): δ 0.94 (t, J = 7, 6H), 1.33 (m, 4H), 1.78−1.85 (m, 4H), 4.14 (m, 4H), 5.04 (s, 4H), 7.39 (m, 4H), 8.42 (s, 2H). ^{13}C NMR (100 MHz, acetone-d_6, 23 °C): δ 13.5, 19.8, 32.4, 49.9, 50.6, 123.6, 124.2, 137.5. HRMS (ESI): m/z 421.1966 ($[M-PF_6]^+$, calcd for $C_{16}H_{28}N_4PF_6$ 421.1950, error 3.2 ppm).

1,2-Bis[*N*-(*N*′-butylimidazolium)]ethane Bis(tetrafluoroborate) (3BF$_4$). Anion-exchange procedure A was used; from **3Br** (1.0 g, 2.3 mmol) and $NaBF_4$ (0.55 g, 5 mmol) in deionized water (10 mL), colorless crystalline **3BF$_4$** (0.91 g, 88%), mp 98.6−100.1 °C, was isolated. ^{1}H NMR (400 MHz, acetone-d_6, 23 °C): δ 0.94 (t, J = 7, 6H), 1.36 (m, 4H), 1.92 (m, 4H), 4.34 (t, J = 7, 4H), 4.97 (s, 4H), 7.74 (t, J = 2, 2H), 7.80 (t, J = 2, 2H), 9.02 (s, 2H). ^{13}C NMR (100 MHz, acetone-d_6, 23 °C): δ 13.7, 20.0, 32.4, 49.7, 50.5, 123.8, 124.1, 137.7. HRMS (ESI): m/z 363.2363 ($[M-BF_4]^+$, calcd for $C_{16}H_{28}N_4BF_4$ 363.2343, error 5.5 ppm).

1,2-Bis[*N*-(*N*′-butylimidazolium)]ethane Bis(triflate) (3TfO). Anion-exchange procedure B was used; from **3Br** (0.30 g, 0.69 mmol) and AgTfO (0.364 g, 1.42 mmol) in deionized water (15 mL), colorless solid **3TfO** (0.384 g, 97%), mp 90.1−93.2 °C, resulted. ^{1}H NMR (400 MHz, acetone-d_6, 23 °C): δ 0.94 (t, J = 7, 6H), 1.38 (m, 4H), 1.92 (m, 4H), 4.35 (t, J = 7, 4H), 5.03 (s, 4H), 7.82 (m, 4H), 9.20 (t, J = 2, 2H). ^{13}C NMR (100 MHz, acetone-d_6, 23 °C): δ 13.6, 20.0, 32.5, 49.8, 50.5, 123.9, 124.1, 137.8. HRMS (ESI): m/z 425.1845 ($[M-TfO]^+$, calcd for $C_{17}H_{28}F_3N_4O_3S$ 425.1834, error 2.6 ppm).

1,2-Bis[*N*-(*N*′-butylimidazolium)]ethane Bis(nitrate) (3NO$_3$). Anion-exchange procedure B was used; from **3Br** (0.30 g, 0.69 mmol) and $AgNO_3$ (0.234 g, 1.42 mmol) in deionizedwater (15 mL), **3NO$_3$** was isolated as a colorless viscous liquid (0.277 g, 97%). ^{1}H NMR (400 MHz, acetone-d_6, 23 °C): δ 0.94 (t, J = 7, 6H), 1.35 (m, 4H), 1.91 (m, 4H), 4.35 (t, J = 7, 4H), 5.02 (s, 4H), 7.78 (t, J = 2, 2H), 7.89 (t, J = 2, 2H), 9.57 (t, J = 2, 2H). ^{13}C NMR (100 MHz, acetone-d_6, 23 °C): δ 13.7, 20.0, 32.5, 49.8, 50.4, 123.8, 124.0, 138.6. HRMS (ESI): m/z 338.2203 ($[M-NO_3]^+$, calcd for $C_{16}H_{28}N_5O_3$ 338.2192, error 3.3 ppm).

1,2-Bis[*N*-(*N*′-butylimidazolium)]ethane Bis(trifuoroacetate) (3TFA). Anion-exchange procedure B was used; from **3Br** (0.30 g, 0.69 mmol) and AgTFA (0.348 g, 1.42 mmol) in deionized water (15 mL), yellow crystalline **3TFA** (0.348 g, 91%), mp 131.7−134.6 °C, resulted. ^{1}H NMR (400 MHz, acetone-d_6, 23 °C): δ 0.93 (t, J = 7, 6H), 1.33 (m, 4H), 1.91 (m, 4H), 4.32 (t, J = 7, 4H), 5.12 (s, 4H), 7.75 (t, J = 2, 2H), 8.14 (t, J = 2, 2H), 10.09 (t, J = 2, 2H). ^{13}C NMR (100 MHz, acetone-d_6, 23 °C): δ 13.6, 19.9, 32.5, 49.2, 50.3, 123.3, 124.3, 139.1. HRMS (ESI): m/z 389.2173 ($[M-CF_3CO_2]^+$, calcd for $C_{18}H_{28}F_3N_4O_2$ 389.2164, error 2.3 ppm).

1,3-Bis[*N*-(*N*′-butylimidazolium)]propane Bis(hexafluorophosphate) (4PF$_6$). The same procedure as for **1Br** was used, except the product could not be filtered because it was a viscous oil. From 1-butylimidazole (3.73 g, 30 mmol) and 1,3-dibromopropane (3.03 g, 15 mmol) in MeCN (20 mL), a light brown viscous liquid **4Br** (5.81 g, 86%) was isolated. ^{1}H NMR (400 MHz, D_2O, 23 °C): δ 0.92 (t, J = 7, 6H), 1.31 (m, 4H), 1.84 (m, 4H), 2.54 (m, 2H), 4.20 (t, J = 7, 4H), 4.33 (t, J = 7, 2H), 7.53 (m, 4H), 8.86 (s, 2H). Anion-exchange procedure A was used for **4PF$_6$**; from **4Br** (5.00 g, 11.1 mmol) and **KPF$_6$** (6.20 g, 33 mmol) in deionized water (40 mL) colorless crystalline solid **4PF$_6$** (6.25 g, 97% from **4Br**), mp 96.4−97.7 °C, resulted.^{1}H NMR (400 MHz, acetone-d_6, 23 °C): δ 0.94 (t, J = 7, 6H), 1.38 (m, 4H), 1.94 (m, 4H), 2.74 (m, 2H), 4.36 (t, J = 7, 4H), 4.55 (t, J = 7, 2H), 7.81 (m, 4H), 9.12 (s, 2H). ^{13}C NMR (100 MHz, acetone-d_6, 23 °C): δ 13.6, 20.0, 31.5, 32.6, 47.5, 50.4, 123.6, 123.9, 136.9. HRMS (ESI): m/z 435.2143 ($[M-PF_6]^+$, calcd for $C_{17}H_{30}N_4PF_6$ 435.2112, error 7.1 ppm).

1,4-Bis[N-(*N*′-butylimidazolium)]butane Bis(hexafluorophosphate) (5PF$_6$). The same procedure as for **4Br** was used; from 1-butylimidazole (3.73 g, 30 mmol) and 1,4-dibromobutane (3.24 g, 15 mmol) in MeCN (20 mL), **5Br** was obtained as a light brown viscous liquid (5.71 g, 82%). Anion-exchange procedure A was used for **5PF$_6$**; from **5Br** (5.70 g, 2.3 mmol)

and KPF_6 (5.56 g, 30 mmol) in deionized water (40 mL) **5PF$_6$** was isolated as an off-white viscous liquid (7.05 g, 96% from **5Br**) which solidified in a vacuum oven, mp 50.4−52.4 °C.^{1}H NMR (400 MHz, CD_3CN, 23 °C): δ 0.94 (t, J = 7, 6H), 1.34 (m, 4H), 1.78−1.85 (m, 8H), 2.74 (m, 4H), 4.14 (m, 8H), 7.38 (m, 4H), 8.42 (s, 2H). ^{13}C NMR (100 MHz, CD_3CN, 23 °C): δ 13.7, 20.0, 27.2, 32.5, 49.8, 50.4, 123.4, 123.6, 136.3. HRMS (ESI): m/z 449.2304 ($[M-PF_6]^+$, calcd for $C_{18}H_{32}N_4PF_6$ 449.2269, error 7.9 ppm).

1-Hexylimidazole. To a solution of imidazole (1.361 g, 20 mmol) in NaOH (50%) solution (0.19 g, 24 mmol), 1-bromohexane (3.31 g, 20 mmol) and THF (15 mL) were added. The mixture was refluxed for three days. After the mixture had cooled to room temperature, THF was removed by a rotoevaporator. The residue was extracted with dichloromethane/water three times. The combined organic layer was washed with water and then dried over Na_2SO_4. The drying agent was filtered off, and the filtrate solution was concentrated. Drying in a vacuum oven gave a yellow oily product, 2.64 g (87%). ^{1}H NMR (400 MHz, $CDCl_3$, 22 °C): δ 0.88 (t, J = 7, 3H), 1.29 (s (br), 6H), 1.77 (m, 2H), 3.92 (t, J = 7, 2H), 6.90 (s, 1H), 7.05 (s, 1H), 7.46 (s, 1H). The ^{1}H NMR spectrum was exactly identical to the literature result.[35]

1,2-Bis[*N*-(*N*′-hexylimidazolium)]ethane Dibromide (6Br). The same procedure as for **1Br** was used. From 1-hexylimidazole (1.52 g, 10 mmol) and 1,2-dibromoethane (0.940 g, 5 mmol) in MeCN (10 mL), colorless crystalline **6Br** (2.14 g, 87%) was isolated, mp 225.5−229.3 °C (dec.). ^{1}H NMR (400 MHz, D_2O, 23 °C): δ 0.71 (t, J = 7, 6H), 1.12 (m, 12H), 1.68 (m, J = 7, 4H), 4.04 (t, J = 8, 4H), 4.79 (overlapped with solvent residual peak), 7.34 (s, 2H), 7.45 (s, 2H), 8.68 (s, 2H). ^{13}C NMR (100 MHz, D_2O, 23 °C): δ 13.4, 21.9, 25.1, 29.0, 30.4, 49.0, 50.2, 123.8, 124.0, 136.0. HRMS (ESI): m/z 411.2132 ($[M-Br]^+$, calcd for $C_{20}H_{36}N_4Br$ 411.2123, error 2.2 ppm).

1,2-Bis[*N*-(*N*′-hexylimidazolium)]ethane Bis(tetrafluoroborate) (6BF$_4$). Anion-exchange procedure A was used; the precipitated oil was washed with water five times and then dried in a vacuum oven. From **6Br** (1.0 g, 2.0 mmol) and $NaBF_4$ (0.66 g, 6 mmol) in deionized water (10 mL), **6BF$_4$** was isolated as a colorless viscous material (0.80 g, 78%). ^{1}H NMR (400 MHz, acetone-d_6, 23 °C): δ 0.87 (t, J = 7, 6H), 1.33 (m, 12H), 1.97 (m, J = 7, 4H), 4.33 (t, J = 8, 4H), 4.94 (s, 4H), 7.72 (s, 2H), 7.76 (s, 2H), 9.00 (s, 2H). ^{13}C NMR (100 MHz, acetone-d_6, 22 °C): δ 14.1, 22.9, 26.3, 30.3, 31.8, 49.9, 50.8, 123.6, 124.1, 137.1. HRMS (ESI): m/z 419.2991 ($[M-BF_4]^+$, calcd for $C_{20}H_{36}N_4BF_4$ 419.2969, error 5.2 ppm).

1,2-Bis[*N*-(*N*′-hexylimidazolium)]ethane Bis(hexafluorophosphate) (6PF$_6$). Anion-exchange procedure A was used; from **6Br** (0.630 g, 1.3 mmol) and KPF_6 (0.56 g, 3.0 mmol) in deionized water (5 mL), colorless crystalline **6PF$_6$** (0.810 g, 91%), mp 197.5−198.8 °C, was isolated. ^{1}H NMR (400 MHz, acetone-d_6, 22 °C): δ 0.87 (t, J = 7, 6H), 1.33 (m, 12H), 1.94 (m, J = 7, 4H), 4.34 (t, J = 8, 4H), 5.01 (s, 4H), 7.74 (s, 2H), 7.87 (s, 2H), 9.04 (s, 2H). ^{13}C NMR (100 MHz, acetone-d_6, 22 °C): δ 14.1, 23.0, 26.4, 30.5, 31.8, 49.9, 50.8, 123.7, 124.3, 137.3. HRMS (ESI): m/z 477.2603 ($[M-PF_6]^+$, calcd for $C_{20}H_{36}N_4PF_6$ 477.2582, error 4.4 ppm).

1,2-Bis[*N*-(*N*′-hexylimidazolium)]ethane Bis[bis(trifluoromethanesulfonyl)imide] (6TFSI). The same procedure as for **6BF$_4$** was used. From **6Br** (0.492 g, 1.0 mmol) and $LiTf_2N$ (0.86 g, 3.0 mmol) in deionized water (5 mL), **6TFSI** was isolated as a colorless viscous oil (0.810 g, 91%). ^{1}H NMR (400 MHz, acetone-d_6, 22 °C): δ 0.87 (t, J = 7, 6H), 1.32 (m, 12H), 1.97 (m, J = 7, 4H), 4.36 (t, J = 8, 4H), 5.08 (s, 4H), 7.73 (s, 2H), 7.96 (s, 2H), 9.11 (s, 2H). ^{13}C NMR (100 MHz, acetone-d_6, 22 °C): δ 14.1, 23.0, 26.3, 30.4, 31.7, 49.8, 50.7, 123.6, 124.2, 137.3. HRMS (ESI): m/z 612.2155 ($[M-Tf_2N]^+$, calcd for $C_{22}H_{36}F_6N_5O_4S_2$ 612.2113, error 4.2 ppm).

1-Dodecylimidazole. To a solution of imidazole (6.81 g, 100 mmol) in NaOH (50%) solution (8.80 g, 110 mmol), 1-bromododecane (24.92 g, 100 mmol) and THF (30 mL) were added. The mixture was refluxed for three days. After the mixture had cooled, THF was removed on a rotoevaporator. The residue was extracted with dichloromethane/water three times. The combined organic layer was washed with water and then dried over Na_2SO_4. The drying agent was filtered off, and the filtrate solution was concentrated. Column chromatography through a short silica-gel column with THF gave a clear yellow oil (20.51 g, 87%). ^{1}H NMR (400 MHz, $CDCl_3$, 22 °C): δ 0.88 (t, J = 7, 3H), 1.29 (m, 18H), 1.76 (m, J = 7, 2H), 3.91 (t, J = 7, 4H), 6.90 (s, 1H), 7.05 (s, 1H), 7.45 (s, 1H). ^{13}C NMR (100 MHz, $CDCl_3$, 22 °C): δ 14.0, 22.6, 26.4, 29.0, 29.2, 29.3, 29.4, 29.5, 31.0, 31.8, 46.9, 118.6, 129.2, 136.9. The ^{1}H NMR spectrum was exactly identical to the literature result.[35]

1,2-Bis[*N*-(*N*′-dodecylimidazolium)]ethane Salts (7Br, 7PF$_6$ and 7TFSI). A solution of 1-dodecylimidazole (3.78 g, 16 mmol) and 1,2-dibromoethane (1.50 g, 8 mmol) in MeCN (15 mL) was refluxed for three days. After the mixture had cooled, the volatile materials were removed by vacuum. The residue was dispersed in THF (30 mL), and the insoluble bromide salt was filtered. The filter cake was washed with THF three times. Drying in a vacuum oven gave a colorless crystalline solid **7Br** (4.54 g, 86%), mp 249.3−252.9 °C (dec). ^{1}H NMR (400 MHz, DMSO-d_6, 23 °C): δ 0.86 (t, J = 7, 6H), 1.25 (m (br), 36H), 1.74 (t, J = 7, 4H), 4.13 (t, J = 7, 4H), 4.71 (s, 4H), 7.69 (s, 2H), 7.85 (s, 2H), 9.15 (s, 2H). HRMS (ESI): m/z 499.4739 ($[M-H-2Br]^+$, calcd for $C_{32}H_{59}N_4$ 499.4740, error 0.2 ppm), m/z 250.7419 ($[M-2Br+H]^{2+}$, calcd for half mass of $C_{32}H_{60}N_4$ 250.7443, error 9.4 ppm). **7PF$_6$** was obtained by following general anion-exchange procedure A, except that the mixture was stirred at 50 °C for 24 h; from **7Br** (2.00 g, 3.03 mmol), KPF_6 (1.56 g, 8.5 mmol), and deionized water (60 mL), colorless solid **7PF$_6$** (2.33 g, 97%), mp 217.4−223.0 °C (dec.), was isolated. ^{1}H NMR (400 MHz, acetone-d_6, 23 °C): δ 0.87 (t, J = 7, 6H), 1.27−1.36 (m (br), 36H), 1.95 (t, J = 7, 4H), 4.35 (t, J = 7, 4H), 5.03 (s, 4H), 7.73 (t, J = 2, 2H), 7.85 (t, J = 2, 2H), 9.03 (s, 2H). ^{13}C NMR (100 MHz, acetone-d_6, 23 °C): δ 14.3, 23.3, 26.8, 29.7, 30.0, 30.1, 30.30, 30.35, 30.36, 32.6, 50.1, 50.9, 123.8, 124.4, 137.4. HRMS (ESI): m/z 645.4465 ($[M-PF_6]^+$, calcd for $C_{32}H_{60}N_4PF_6$ 645.4460, error 0.8 ppm). For **7TFSI**, the same procedure as for **7PF$_6$** was used. From **7Br** (2.70 g, 6.4 mmol), $LiTf_2N$ (4.32 g, 15 mmol), and deionized water (60 mL), crystalline **7TFSI** (3.89 g, 97% from **7Br**), mp 45.5−47.7 °C, was isolated. ^{1}H NMR (400 MHz, $CDCl_3$, 23 °C): δ 0.87 (t, J = 7, 6H), 1.25−1.31 (m (br), 36H), 1.86 (t, J = 7, 4H), 4.15 (t, J = 7, 4H), 4.74 (s, 4H), 7.33 (t, J = 2, 2H), 7.60 (t, J = 2, 2H), 8.84 (s, 2H). ^{13}C NMR (100 MHz, $CDCl_3$, 23 °C): δ 14.2, 22.8, 26.3, 29.0, 29.4, 29.5, 29.6, 29.7, 32.0, 48.5, 50.7, 123.0, 123.3, 136.0. HRMS (ESI): m/z 780.3997 ($[M-Tf_2N]^+$, calcd for $C_{34}H_{60}F_6N_5O_4S_2$ 780.3985, error 0.8 ppm).

Results and Discussion

Various alkylene bis[*N*-(*N*′-alkylimidazolium)] salts were synthesized in two steps (Scheme 1): the coupling reaction of the 1-alkylimidazole (2 mol equiv) with a dibromoalkane (1 mol equiv) and anion exchange in water. Noncommercial

SCHEME 1: Synthesis of Alkylene bis[*N*-(*N*′-alkylimidazolium)] Salts

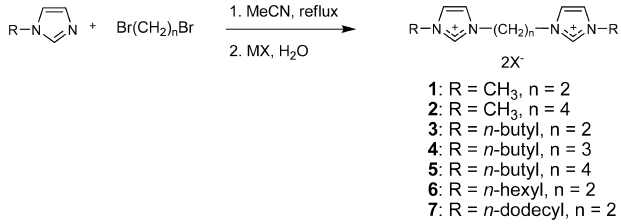

TABLE 1: Quaternization and Ion-Exchange Reactions for Alkylene Bis[*N*-(*N*′-alkylimidazolium)] Salts

R	*n*	quaternization yield (%, *X* = Br)	*X*	ion exchange yield (%)	appearance
Me					
	2	86	PF_6	92	Crst. Solid
	4	53[a]	PF_6	92	Crst. Solid
n-Bu					
	2	88	PF_6	91	Crst. Solid
	2		BF_4	88	Crst. Solid
	2		TfO	97	Crst. Solid
	2		NO_3	96	RTIL[b]
	2		CF_3CO_2	97	Yellow Solid
	3	86	PF_6	96	Crst. Solid
	4	82	PF_6	96	Sticky Solid
n-Hex					
	2	87	PF_6	91	Solid
	2		BF_4	88	RTIL[b]
	2		Tf_2N	90	RTIL[b]
n-Dodecyl					
	2	82	PF_6	97	Crst. Solid
	2		Tf_2N	89	Crst. Solid

[a] The yield was lower than that for other reactions because of a higher solubility of **2Br** in MeCN during the workup procedure. [b] RTIL = room temperature IL.

1-alkylimidazoles were first prepared before the quaternization; 1-hexylimidazole and 1-dodecylimidazole were prepared from imidazole and corresponding bromoalkanes with NaOH in high yields.[10]

Most of the alkylene *N*-(*N*′-alkylimidazolium) bromide salts were very hygroscopic; they are either crystalline solids or waxy materials. The counteranion exchange was performed in aqueous conditions with $NaBF_4$, KPF_6, or $(CF_3SO_2)_2NLi$ (denoted Tf_2NLi or LiTFSI), and the resulting products (BF_4^-, PF_6^-, and Tf_2N^- salts) precipitated, as solids or liquids. The BF_4^-, PF_6^-, and Tf_2N^- salts are not hygroscopic because of their hydrophobic anions. The triflate (TfO^-), nitrate, and trifluoroacetate (TFA) salts were prepared from the corresponding Ag salts in water; AgBr precipitation provided the driving force to complete the ion-exchange reactions. The triflate, nitrate, and TFA salts are water-soluble and as hygroscopic as the bromide salts. The results of the quaternizaton and anion-exchange reactions for the alkylene bis[*N*-(*N*′-alkylimidazolium)] salts are summarized in Table 1.

^{1}H NMR Studies. In our ^{1}H NMR studies of the new bis[*N*-(*N*′-alkylimidazolium)] salts, noteworthy chemical-shift changes were observed with different solvents and counterions. The ^{1}H NMR spectra of the bromide salt of **3** (**3Br**) in D_2O and acetone-d_6 are shown in Figure 1. The imidazolium protons appear at different positions in these solvents: δ 7.5, 7.6, and 8.9 in D_2O but δ 7.7, 8.4, and 10.4 in acetone-d_6. The peaks of H^4 and H^5 are close to each other in D_2O, but they are widely separated in acetone-d_6. These chemical-shift changes are due to the solvent properties: the better solvation of the ions in D_2O versus acetone-d_6. This higher solvation level isolates the bromide anions in solution, and the positive charge on the resultant free cation is delocalized. As a result of the delocalization of positive charge, the chemical shifts of protons H^4 and H^5 are close to each other. However, poorer ion solvation in acetone-d_6 results in relatively tight ion pairs; therefore, the positive charge tends to localize on a specific nitrogen atom. The localized positive charge leads to different environments for protons H^4 and H^5, and hence, their peaks occur at different positions.

The chemical-shift change of proton H^2 is quite large in different media: δ 8.9 (D_2O) versus 10.4 (acetone-d_6). This can be explained by the different solvating powers of the solvents. In D_2O, the imidazolium cations and bromide anions are well solvated, and hydrogen bonding of proton H^2 with the bromide anion is decreased, thus moving its signal to higher field. However, hydrogen bonding occurs in the less polar acetone-d_6, in which the ions are rather tightly paired; therefore, in acetone-d_6, the proton H^2 appears downfield. The chemical-shift changes of bromide salts of (mono)imidazolium ILs in different solvents were reported previously,[36] and those results are consistent with our study of bis(imidazolium) bromide **3Br**.

There is a counteranion effect on the chemical shifts of the imidazolium protons as shown in Figure 2. The hydrogen-bonding abilities of the different anions influence the NMR chemical shifts. In this series, the bromide salt (**3Br**) showed the strongest hydrogen bonds, and the PF_6^- and BF_4^- salts (**3PF$_6$** and **3BF$_4$**) showed the least hydrogen bonding in acetone-d_6. The chemical shift of H^2 (**a**) increased with increasing anion basicity and hydrogen bonding ability ($PF_6^- \approx BF_4^- < TfO^- < NO_3^- \ll Br^-$).[37] The different ion-pairing strengths[38−40] of the anions were also observed from the chemical-shift changes of H^4 and H^5. The most ion-paired salt (**3Br**) showed the largest difference in the chemical shifts of these protons, whereas the least ion-paired salts gave more closely spaced (**3TFA**, **3NO$_3$**, **3BF$_4$**, **3PF$_6$**) or merged peaks (**3TfO**). These changes are the result of changes in the charge

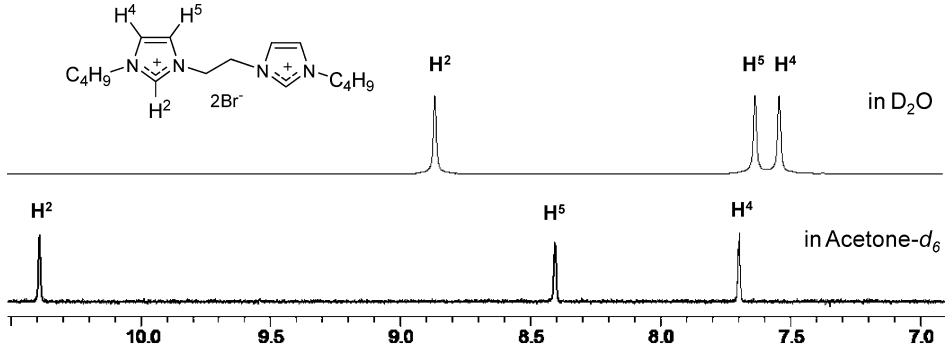

Figure 1. Partial 400 MHz ^{1}H NMR spectra of **3Br** in D_2O (upper) and acetone-d_6 (lower).

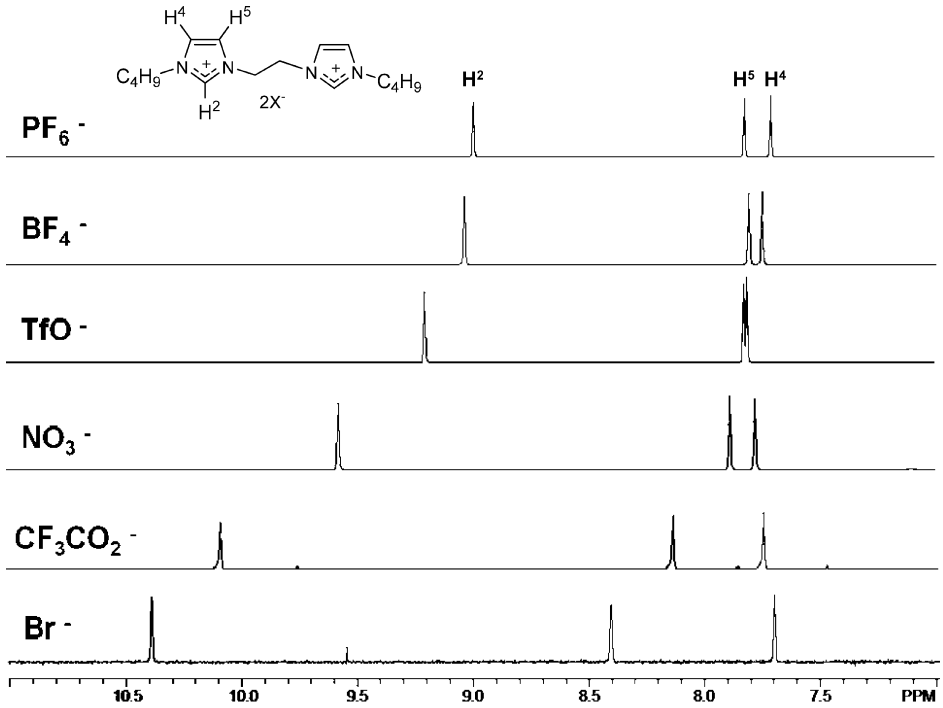

Figure 2. Partial 400 MHz ^{1}H NMR spectra of **3** (PF_6^-, BF_4^-, TfO^-, NO_3^-, TFA, and Br^-) in acetone-d_6. The chemical shift of proton H^4 is almost the same with various anions, but protons H^2 and H^5 resonate at different positions. **3PF$_6$** and **3BF$_4$** are the least ion-paired, bringing the signals of protons H^4 and H^5 close to each other. **3Br** is the most ion-paired; the positive charge is localized in the imidazolium ring.

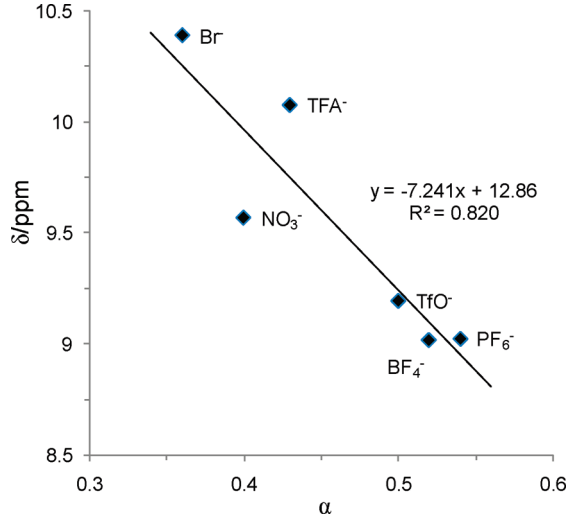

Figure 3. Correlation of the ^{1}H chemical shift of the proton in 2-position of the imidazolium ring of **3** with the hydrogen-bond acidity (α) of 1-butyl-3-methylimidazolium salts.[41]

localization/delocalization and hydrogen bonding with the different anions.

The correlation of the ^{1}H NMR chemical shifts of H^2 of 1-butyl-3-methylimidazolium salts with hydrogen bonding was reported by Spange et al.[41] They calculated hydrogen bond acidities (α) of 1-butyl-3-methylimidazolium salts by UV/vis spectrometry with an indicator dye as a probe. Because half of the imidazolium salts **3** corresponds to the 1-butyl-3-methylimidazolium salts, we directly adapt the α values from the literature and use them to correlate the proton H^2 chemical shifts (Figure 3). Even though the NMR spectra were taken in different solvents (CD_2Cl_2 in the literature[41] and acetone-d_6 in this work), the correlation plot is similar to the literature result; the r^2 of the trend line is 0.82, which is close to the literature result, 0.83. This result reflects the fact that the acidity changes through different anions are similar between the C2 proton of the 1,2-bis[*N*-(*N*′-butylimidazolium)ethane salts **3** and that of 1-butyl-3-methylimidazolium salts.

Thermal Properties. From this study, structural factors were found to affect the melting points and thermal stabilities of the alkylene bis(alkylimidazolium) salts: (1) alkyl substituent, (2) the length of the spacer between two imidazolium dications, and (3) the nature of the anion.

When we compare the melting points of the PF_6^- salts of 1,2-bis[*N*-(*N*′-alkylimidazolium)]ethanes, **7PF$_6$**, which has C_{12} termini, has the highest melting point but decomposes upon melting. The decreasing order of melting points is didodecyl **7PF$_6$** > dimethyl **1PF$_6$** > dihexyl **6PF$_6$** > dibutyl **5PF$_6$**. The

TABLE 2: Thermal Properties of the Alkylene Bis(*N*-alkylimidazolium) Salts

entry	side chain	spacer	MP (°C)[a]	TGA 5% weight loss (°C)
1PF$_6$	Me	C_2	214.3	304
2Br	Me	C_4	132.8	250
2PF$_6$	Me	C_4	112.9	342
3Br	Bu	C_2	167.3	252
3PF$_6$	Bu	C_2	182.0	273
3BF$_4$	Bu	C_2	99.4	298
3TfO	Bu	C_2	91.6	331
3NO$_3$	Bu	C_2	—[b]	161
3TFA	Bu	C_2	133.2	156
4PF$_6$	Bu	C_3	96.1	326
5PF$_6$	Bu	C_4	51.3	335
6Br	Hex	C_2	227.4 (dec.)	231
6PF$_6$	Hex	C_2	198.2	239
7Br	Dodecyl	C_2	240.6 (dec.)	240
7PF$_6$	Dodecyl	C_2	220.4 (dec.)	285
7TFSI	Dodecyl	C_2	46.6	334

[a] Median values from the melting (or decomposition) ranges. Melting points were observed with a Büchi B-540 apparatus at a 2 °C/min heating rate. [b] No melting point because **3NO$_3$** is an RTIL.

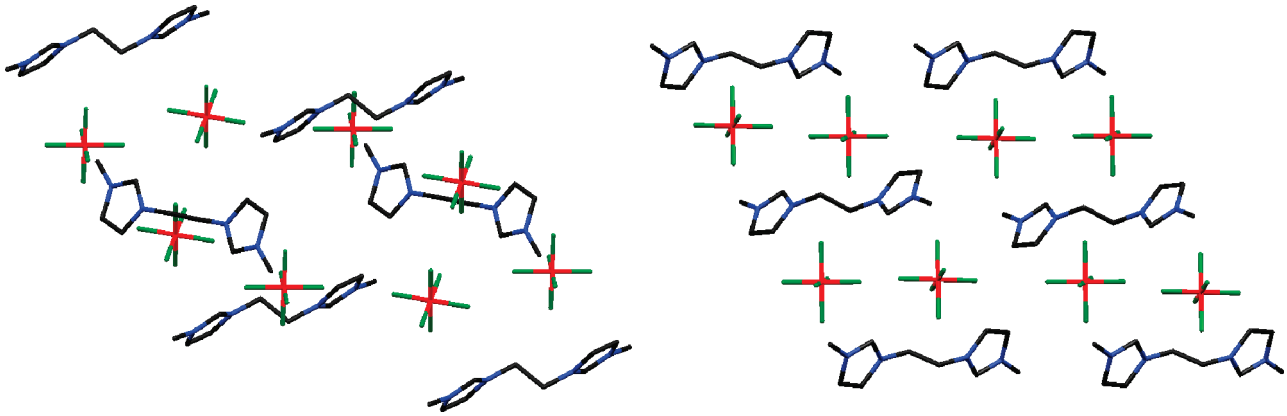

Figure 4. Two capped-sticks views of the X-ray structure of **1PF$_6$**. Hydrogens are omitted for clarity. Face-to-face stacking parameters: ring plane/ring plane inclination of the imidazolium rings in the same molecule, 0°. Ring plane/ring plane distance and dihedral angle between imidazolium rings of different molecules within a stack, 8.66 Å, 0°. Dihedral angle between imidazolium rings in different stacks, 67.3°.

melting points of Br^- salts with C_2 spacer decrease as follows: didodecyl **7Br** > dihexyl **6Br** > dibutyl **3Br**.

The spacer length between the imidazolium cations plays an important role. The melting point of dimethyl **2PF$_6$** with a C_4 spacer is 100° lower than the melting point of dimethyl **1PF$_6$** with a C_2 spacer. Similarly, dibutyl **3PF$_6$** with a C_2 spacer melts 86° higher than dibutyl**4PF$_6$** with a C_3 spacer and 131° higher than dibutyl**5PF$_6$** with a C_4 spacer. These results are consistent with the literature.

To see the effect of the anions, the bis(imidazolium)ethanes were compared. The melting points increased in the following order: **3TfO** < **3BF$_4$** < **3TFA** < **3Br** < **3PF$_6$**. (**3NO$_3$** falls below all of these because it is an RTIL.) This order is somewhat different from previously reported systems with longer spacers (C_3 to C_{12}) between the imidazolium units; in these systems, the melting points of the bromide salts were usually higher than the PF_6^- salts.[28]

The thermal stabilities of the alkylene bis(*N*-alkylimidazolium) salts were investigated by thermal gravimetric analysis (TGA) in N_2 atmosphere. All the imidazolium salts evinced one step degradation; the 5% weight-loss temperatures are shown in Table 2. For the 1,2-bis(alkylimidazolium)ethane PF_6 salts, the thermal stabilities are in the following order: dimethyl **1PF$_6$** > dibutyl **3PF$_6$** ≫ didodecyl **7PF$_6$** > dihexyl **6PF$_6$**. The Br^- salts showed a similar order: dibutyl **3Br** > didodecyl **7Br** > dihexyl **6Br**.

The thermal stability was also affected by the spacer length. For the salts with methyl arms, **2PF$_6$** with a C_4 spacer has better thermal stability than **1PF$_6$** with a C_2 spacer. The dibutyl analogues behave similarly. In the dibutyl series, **5PF$_6$** with a C_4 spacer > **4PF$_6$** with a C_3 spacer > **3PF$_6$** with a C_2 spacer. The literature reported that bis(1-methylimidazolium) $2Tf_2N^-$ with a C_9 spacer started to decompose at ~330 °C,[28] which is slightly higher compared to the degradation of dibutyl **5PF$_6$** with a C_4 spacer and didodecyl **7TFSI** with a C_2 spacer.

The nature of the anion greatly influences the thermal stabilities of the salts of dibutyl **3** with a C_2 spacer. The thermal stability is in the following order: **3TfO** > **3BF$_4$** > **3PF$_6$** > **3Br** > **3NO$_3$** > **3TFA**. This thermal stability order is almost the same as that of the basicity of anions; the more basic TFA^- and NO_3^- salts degrade at relatively low temperatures. However, the imidazolium salts containing less basic counterions show good thermal stabilities.

Solid-State Structures of 1PF$_6$, 3PF$_6$. Crystals of **1PF$_6$** and **3PF$_6$** were obtained by vapor-diffusion methods. The crystal structure of **1PF$_6$**[42] (Figure 4) reveals that the planar imidazolium rings are parallel in each molecule. There are two sets of stacks in the unit cell; the imidazolium rings are arranged at an angle of 67.3° to one another in the two stacks, that is, a herringbone structure. Surprisingly, every proton of **1PF$_6$** is within hydrogen-bonding distance of a fluorine atom of PF_6^- anions (Figure 5). The H···F distances are in the range of 2.31−2.69 Å. The shortest H···F distance is **A** (2.31 Å) for the most acidic proton, H^2, of the imidazolium cation.

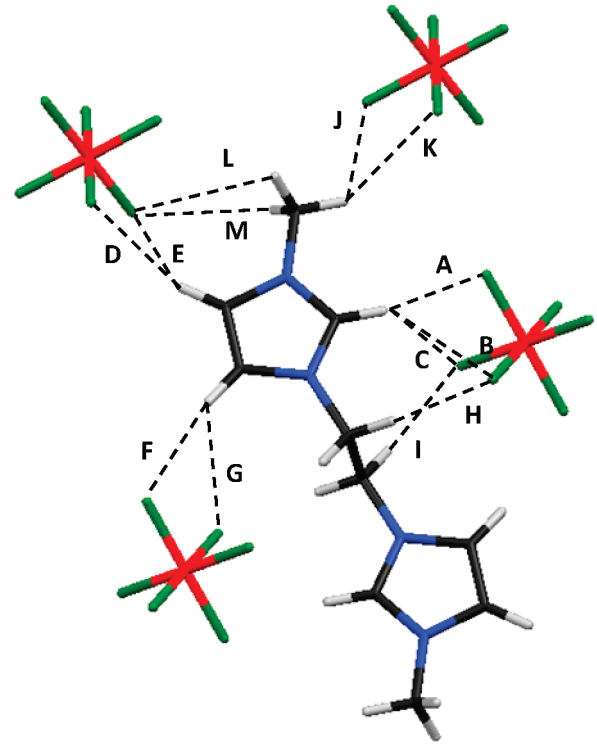

Figure 5. Capped-sticks view of the X-ray structure of **1PF$_6$**. H···F distances (Å), C−H···F angles (degrees): **A** 2.31, 166; **B** 2.58, 137; **C** 2.78, 126; **D** 2.48, 159; **E** 2.71, 130; **F** 2.69, 164; **G** 2.66, 126; **H** 2.52, 125; **I** 2.50, 164; **J** 2.56, 112; **K** 2.60, 146; **L** 2.65, 123; **M** 2.84, 122.

The crystal structure of dibutyl **3PF$_6$**[45] (Figure 6) contains only one type of stacking; that is, the structure is of higher symmetry than **1PF$_6$**. The two imidazolium rings of the molecule are exactly parallel. The two imidazolium ring planes of neighboring molecules are also exactly parallel. There are also many apparent hydrogen bonds in the solid state. The shortest H···F distance is 2.26 Å for H^2, and the C−H···F angle is 175°. The H···F distances for H^3 and H^4 are 2.23 and 2.42 Å,

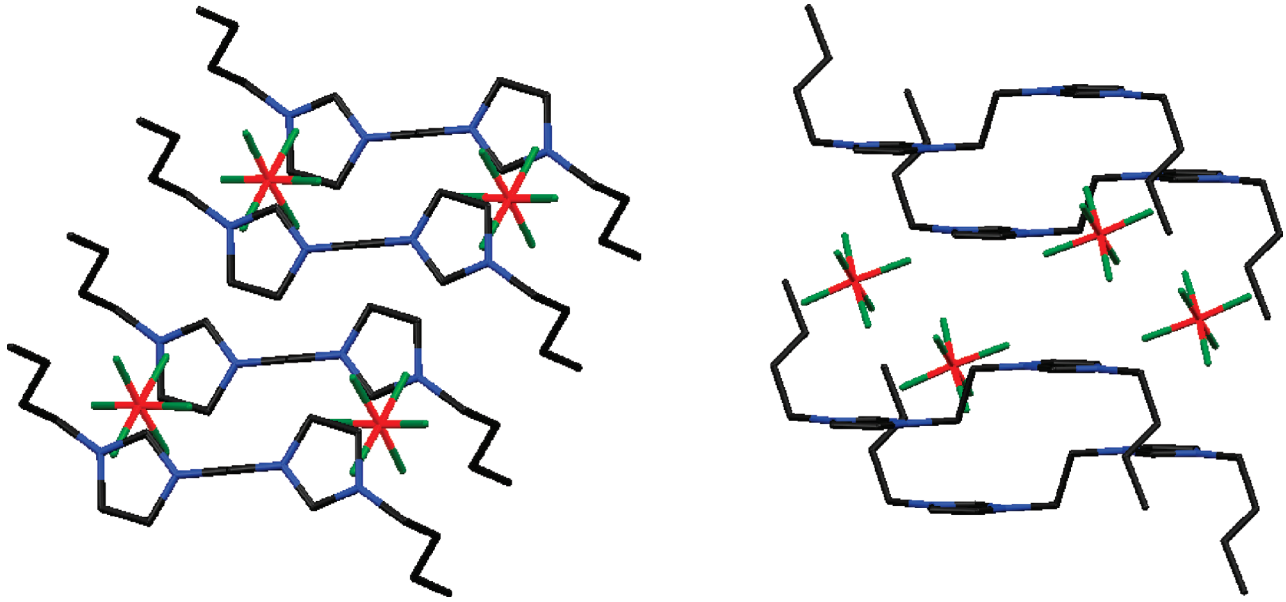

Figure 6. Two capped-sticks views of the X-ray structure of **3PF$_6$**. Hydrogens are omitted for clarity. Face-to-face stacking parameters: ring plane/ring plane inclination of imidazolium rings within the same molecule, 0°. Ring plane/ring plane distance and dihedral angle between imidazolium rings of different molecules, 7.94 Å, 0°.

respectively. The H···F distances for the ethylene protons are 2.41 and 2.52 Å.

We can rationalize the high melting points of the PF_6^- salts with C_2 spacers from the solid-state structures. Because of the octahedral geometry of the PF_6^- anion, two or three fluorine atoms are bound to one cation, and the other three are bound to the neighboring cations (Figure 5); in this way, each cation is linked to its neighbors. The lower melting points of BF_4^- (tetrahedral) and TFSI (asymmetric) salts are probably due to weaker and fewer hydrogen bonds provided by these lower symmetry anions.

Conclusions

A series of alkylene bis[*N*-(*N*′-alkylimidazolium)] salts with various anions was prepared in high yields. The hydrogen bonding and ion pairing of the salts in solution were characterized by ^{1}H NMR. Chemical shift changes of the C2 proton result from changes in solvent and anion. For the bromide salts, the hydrogen bonding of H^2 with the counterion was more pronounced in acetone-d_6 than in D_2O. The hydrogen-bonding ability was also related to the basicity of the anion ($Br^- > TFA^- > NO_3^- > TfO^- \geq BF_4^- \approx PF_6^-$). Thermal properties of the salts were investigated by their melting points and TGA. The spacers affect the melting points and thermal stabilities. The C_2 spacer salts show higher melting points and lower thermal stabilities than C_3 and C_4 spacer analogues. The length of alkyl side arms does have a significant effect on the thermal properties. Also, the effect of the anions is significant. Better thermal stability was shown with the less nucleophilic anions: $TfO^- > BF_4^- > PF_6^- > Br^- > NO_3^- > TFA^-$. The PF_6^- salts of 1,2-bis[*N*-(*N*′-alkylimidazolium)]ethane surprisingly possess high melting points; this is attributed to the multiple hydrogen bonds of the imidazolium units with fluorine atoms of PF_6^-, as directly observed in X-ray crystal structures. The two imidazolium rings in the same molecule are parallel because of the *trans* conformation of the ethylene spacer. The multiple hydrogen bonds and the *trans* conformation also provide well-ordered stacks in their X-ray crystal structures.

Acknowledgment. This material is based upon work supported in part by the U.S. Army Research Office under grant number W911NF-07-1-0452, ILs in Electro-Active Devices (ILEAD) MURI. We thank the National Science Foundation for funds to purchase the Varian Unity and Inova NMR spectrometers (DMR-8809714 and CHE-0131124), the Agilent 6220 Accurate Mass TOF LC/MS Spectrometer (CHE-0722638), and the Oxford Diffraction SuperNova X-ray diffractometer (CHE-0131128). We are grateful to Prof. James McGrath and Prof. Timothy Long (VPI&SU) for use of their thermal analysis equipment.

Supporting Information Available: NMR spectra for all synthesized compounds and X-ray crystallographic data. This material is available free of charge via the Internet at http://pubs.acs.org.

References and Notes

(1) Wolfgang, A. H.; Martina, E.; Jakob, F.; Christian, K. H.; Georg, R. J. A. *Chem.—Eur. J.* **1996**, *2*, 772–780.
(2) Douthwaite, R. E.; Green, M. L. H.; Silcock, P. J.; Gomes, P. T. *Organometallics* **2001**, *20*, 2611–2615.
(3) Lee, K. M.; Wang, H. M. J.; Lin, I. J. B. *J. Chem. Soc., Dalton Trans.* **2002**, 2852–2856.
(4) Lee, H. M.; Lu, C. Y.; Chen, C. Y.; Chen, W. L.; Lin, H. C.; Chiu, P. L.; Cheng, P. Y. *Tetrahedron* **2004**, *60*, 5807–5825.
(5) Mata, J. A.; Chianese, A. R.; Miecznikowski, J. R.; Poyatos, M.; Peris, E.; Faller, J. W.; Crabtree, R. H. *Organometallics* **2004**, *23*, 1253–1263.
(6) Chiu, P. L.; Chen, C. Y.; Zeng, J. Y.; Lu, C. Y.; Lee, H. M. *J. Organomet. Chem.* **2005**, *690*, 1682–1687.
(7) Morvan, D.; Capon, J.-F.; Gloaguen, F.; Le Goff, A.; Marchivie, M.; Michaud, F.; Schollhammer, P.; Talarmin, J.; Yaouanc, J.-J.; Pichon, R.; Kervarec, N. *Organometallics* **2007**, *26*, 2042–2052.
(8) Wells, K. D.; Ferguson, M. J.; McDonald, R.; Cowie, M. *Organometallics* **2008**, *27*, 691–703.
(9) Jia, W. G.; Huang, Y. B.; Lin, Y. J.; Jin, G. X. *Dalton Trans.* **2008**, 5612–5620.
(10) Letaief, S.; Detellier, C. *J. Mater. Chem.* **2007**, *17*, 1476–1484.
(11) Poyatos, M.; Mas-Marza, E.; Sanau, M.; Peris, E. *Inorg. Chem.* **2004**, *43*, 1793–1798.
(12) Bernd, S. *Angew. Chem. Int. Ed.* **2003**, *42*, 4996–4999.
(13) Crabtree, R. H. *Dalton Trans.* **2003**, 3985–3990.
(14) Cavell, K. J.; McGuinness, D. S. *Coord. Chem. Rev.* **2004**, *248*, 671–681.
(15) David, S.; Christian, B.; Pierre, D. *Adv. Synth. Catal.* **2002**, *344*, 585–595.
(16) Ennis, E.; Handy, S. T. *Curr. Org. Syn.* **2007**, *4*, 381–389.
(17) Handy, S. T.; Okello, M. *J. Org. Chem.* **2005**, *70*, 1915–1918.

(18) Wilkes, J. S.; Zaworotko, M. J. *J. Chem. Soc., Chem. Commun.* **1992**, 965–967.
(19) Welton, T. *Chem. Rev.* **1999**, *99*, 2071–2083.
(20) Xu, W.; Cooper, E. I.; Angell, C. A. *J. Phys. Chem. B.* **2003**, *107*, 6170–6178.
(21) Miao, W.; Chan, T. H. *Acc. Chem. Res.* **2006**, *39*, 897–908.
(22) MacFarlane, D. R.; Forsyth, M.; Howlett, P. C.; Pringle, J. M.; Sun, J.; Annat, G.; Neil, W.; Izgorodina, E. I. *Acc. Chem. Res.* **2007**, *40*, 1165–1173.
(23) Plechkova, N. V.; Seddon, K. R. *Chem. Soc. Rev.* **2008**, *37*, 123–150.
(24) Liu, S.; Montazami, R.; Liu, Y.; Jain, V.; Lin, M.; Heflin, J. R.; Zhang, Q. M. *Appl. Phys. Lett.* **2009**, *95*, 023505.
(25) Green, M. D.; Long, T. E. *Polym. Rev.* **2009**, *49*, 291–314.
(26) Brown, R. H.; Duncan, A. J.; Choi, J.-H.; Park, J. K.; Wu, T.; Leo, D. J.; Winey, K. I.; Moore, R. B.; Long, T. E. *Macromolecules* **2010**, *43*, 790–796.
(27) Liu, S.; Liu, W.; Liu, Y.; Lin, J.-H.; Zhou, X.; Janik, M. J.; Colby, R. H.; Zhang, Q. *Polym. Int.* **2010**, *59*, 321–328.
(28) Anderson, J. L.; Ding, R.; Ellern, A.; Armstrong, D. W. *J. Am. Chem. Soc.* **2004**, *127*, 593–604.
(29) Pitawala, J.; Matic, A.; Martinelli, A.; Jacobsson, P.; Koch, V.; Croce, F. *J. Phys. Chem. B* **2009**, *113*, 10607–10610.
(30) Kim, J. Y.; Kim, T. H.; Kim, D. Y.; Park, N.-G.; Ahn, K.-D. *J. Power Sources* **2008**, *175*, 692–697.
(31) Zafer, C.; Ocakoglu, K.; Ozsoy, C.; Icli, S. *Electrochim. Acta* **2009**, *54*, 5709–5714.
(32) Jin, C.-M.; Ye, C.; Phillips, B. S.; Zabinski, J. S.; Liu, X.; Liu, W.; Shreeve, J. M. *J. Mater. Chem.* **2006**, *16*, 1529–1535.
(33) Zeng, Z.; Phillips, B. S.; Xiao, J.-C.; Shreeve, J. M. *Chem. Mater.* **2008**, *20*, 2719–2726.
(34) Varma, R. S.; Namboodiri, V. V. *Chem. Commun.* **2001**, 643–644.
(35) Martin, T.; Sabine, L.; Angelika, B. *Helv. Chim. Acta* **2004**, *87*, 2742–2749.
(36) Lin, S. T.; Ding, M. F.; Chang, C. W.; Lue, S. S. *Tetrahedron* **2004**, *60*, 9441–9446.
(37) Bonhote, P.; Dias, A.-P.; Papageorgiou, N.; Kalyanasundaram, K.; Gratzel, M. *Inorg. Chem.* **1996**, *35*, 1168–1178.
(38) Jones, J. W.; Gibson, H. W. *J. Am. Chem. Soc.* **2003**, *125*, 7001–7004.
(39) Huang, F.; Jones, J. W.; Slebodnick, C.; Gibson, H. W. *J. Am. Chem. Soc.* **2003**, *125*, 14458–14464.
(40) Huang, F.; Jones, J. W.; Gibson, H. W. *J. Org. Chem.* **2007**, *72*, 6573–6576.
(41) Lungwitz, R.; Friedrich, M.; Linert, W.; Spange, S. *New J. Chem.* **2008**, *32*, 1493–1499.
(42) Colorless prisms crystallized from acetone/pentane at room temperature. The chosen crystal was centered on the goniometer of an Oxford Diffraction Gemini A Ultra diffractometer operating with MoKα radiation. The data-collection routine, unit-cell refinement, and data processing were carried out with the program CrysAlisPro.[43] The Laue symmetry and systematic absences were consistent with the monoclinic space groups *C*2/*c* and *Cc*. The centric space group C2/c was chosen on the baiss of the E-statistics. The structure was solved by direct methods and refined by using SHELXTL NT.[44] The asymmetric unit of the structure comprises 0.5 crystallographically independent molecules. The final refinement model involved anisotropic-displacement parameters for non-hydrogen atoms and a riding model for all hydrogen atoms. Crystal data: prism, colorless, crystal size = 0.21 × 0.21 × 0.09 mm^3, $C_{10}H_{16}N_4$•2PF_6, M = 482.21, wavelength = 0.71073 Å, monoclinic, space group C2/c, a = 22.186(3) Å, b = 6.4852(3) Å, c = 14.4065(13) Å, α = 90°, β = 122.621(15)°, γ = 90°, V = 1745.8(3) Å^3, Z = 4, D_c = 1.835 Mg/m3, T = 100(2) K, μ = 0.376 mm^{-1}, 11193 reflections collected, 2562 [R(int) = 0.0300] independent reflections, 2562/0/128 data/restraints/parameters, F(000) = 968, R_1 = 0.0358, wR_2 = 0.0780 (all data), R_1 = 0.0288, wR_2 = 0.0759 [$I > 2\sigma(I)$], and goodness of fit on F2 = 1.051.
(43) *CrysAlisPro v171.33.51*, Oxford Diffraction: Wroclaw, Poland, 2009.
(44) Sheldrick, G. M. *Acta Crystallogr.* **2008**, *A64*, 112–122.
(45) Colorless plates crystallized from acetone/pentane by vapor diffusion. The chosen crystal was centered on the goniometer of an Oxford Diffraction Gemini A Ultra diffractometer operating with MoKα radiation. The data-collection routine, unit-cell refinement, and data processing were carried out with the program CrysAlisPro.[43] The Laue symmetry was consistent with the triclinic space group *P*-1. The structure was solved by direct methods and refined by using SHELXTL NT.[44] The asymmetric unit of the structure comprises 0.5 crystallographically independent formula units. The final refinement model involved anisotropic-displacement parameters for non-hydrogen atoms and a riding model for all hydrogen atoms. The PF_6 anion was modeled with 2-position disorder with relative occupancies that refined to 0.761(9) and 0.239(9). The P−F bond lengths and the F···F distances were restrained with DFIX, and the anisotropic-displacement parameters of the disordered fluorine atoms were restrained with SIMU. Crystal data: plate, colorless, crystal size = 0.03 × 0.18 × 0.47 mm^3, $C_{16}H_{28}N_4$•2PF_6, M = 566.36, wavelength = 0.71073 Å, triclinic, space group P-1, a = 6.5214(3) Å, b = 6.9156(3) Å, c = 13.8874(7) Å, α = 97.336(4)°, β = 97.674(4)°, γ = 99.448(4)°, V = 605.07(5) Å^3, Z = 1, D_c = 1.554 Mg/m3, T = 100(2) K, μ = 0.284 mm^{-1}, 6608 reflections collected, 2795 [R(int) = 0.0338] independent reflections, 2795/60/193 data/restraints/parameters, F(000) = 290, R_1 = 0.0961, wR_2 = 0.1269 (all data), R_1 = 0.0517, wR_2 = 0.1129 [$I > 2\sigma(I)$], and goodness of fit on F2 = 0.989.

JP102370J